Chapter 5

Prescribed-time constrained feedback control for an uncertain twin rotor helicopter

5.1 Introduction

In the previous chapter, we focused on the problem of adaptive prescribed-time control for trajectory tracking of an uncertain nonlinear twin rotor helicopter system. However, we encountered some challenges with the time-varying function gain, which could lead to an infinite control gain as the prescribed time is approached. Moreover, the practical application of the integrator backstepping technique revealed restricted regions in the system states, where the desired virtual controllers might exceed the constraints, causing difficulties in tracking them. To address these issues, this chapter explores an alternative approach, adaptive prescribed-time constrained feedback control, leveraging the tangent hyperbolic function.

The proposed constrained feedback control aims to ensure that the control inputs remain within permissible regions, thus avoiding instability or infeasibility in practical applications. By employing the tangent hyperbolic function, we achieve smooth and bounded control inputs, mitigating the challenges posed by unbounded gains.

The main contributions of this chapter are as follows:

(i) The approach employs an adaptive integrator backstepping technique to design a control law that ensures reference tracking of the system states within a predetermined time frame.

(ii) The approach utilizes adaptive laws to estimate the unknown parameters of the system.

(iii) A constraint function is also utilized to restrict the virtual control signal from becoming excessively large as the prescribed time approaches.

(iv) Through rigorous mathematical analysis, we establish the prescribed-time tracking and boundedness of all signals in the closed-loop twin rotor helicopter system utilizing Lyapunov theory.

The structure of this chapter is outlined as follows. Section 5.2 presents the preliminaries that lay the foundation for obtaining the main results. In Section 5.3, the main results of the study are presented. Section 5.4 focuses on validating the effectiveness of the proposed scheme through simulations and experiments. Finally, in Section 5.5, the chapter concludes the work.

5.2 Preliminaries and problem statement

In this section, we first provide the relevant definitions and lemmas, followed by the presentation of the mathematical model for the considered unmanned twin rotor helicopter.

Definition 5.1 *[110] For the system* (3.1)*, if there exists a control law* $u(t) = u(t, z(t), \hat{\Phi})$ *with the parameter adaptive law* $\dot{\hat{\Phi}} = \psi(t, z(t), \hat{\Phi})$*, where* $\hat{\Phi}$ *is the estimate of* Φ*, such that for any bounded initial condition* $z(0) \in \mathbb{R}^n$*, the trajectories of* $z(t)$ *and* $\hat{\Phi}$ *remain bounded and* $z(t) = 0$ *for all* $t \geq t_p$*, then the origin of system* (3.1) *is said to be prescribed-time stable within the a priori chosen time* t_p*.*

Lemma 5.2 *[110] For the system described by equation* (3.1)*, if there exist two positive definite continuous and differentiable functions* $V_1(z)$ *and* $V_2(\tilde{\Phi})$*, as well as class* $\mathcal{K}_\infty$ *functions* β_1*,* β_2*,* β_3*, and* β_4*, such that for all* $z(t) \in \mathbb{R}^n$*, the following conditions hold:*

$$V = V_1(z) + V_2(\tilde{\Phi}) \tag{5.1}$$

$$\beta_1(\|z\|) \leq V_1(z) \leq \beta_2(\|z\|) \tag{5.2}$$

$$\beta_3(\|\tilde{\Phi}|) \leq V_2(\tilde{\Phi}) \leq \beta_4(\|\tilde{\Phi}\|) \tag{5.3}$$

$$\dot{V} \leq \begin{cases} -\gamma\psi(t, t_p)V_1(z), & \forall t \in [0, t_p) \\ 0, & \forall t \in [t_p, \infty) \end{cases} \tag{5.4}$$

where $\gamma > 1$ *is a design constant and* $\psi(t, t_p)$ *is the prescribed time adjustment function defined in Remark 2.12. Then the origin of the system* (3.1) *is prescribed-time stable and all the closed-loop signals are bounded.*

Definition 5.3 *[110] If a continuous function satisfies $\psi(t, t_p) > 0$ for all $t \in [0, t_p)$ and $\lim_{t \to t_p^-}(t_p - t)\psi(t, t_p) = \nu$, where ν is a positive constant or $+\infty$, then $\psi(t, t_p)$ is called as a prescribed-time adjustment function.*

Remark 5.4 *Please note that the time-varying function $\psi(t, t_p)$ may lead to an infinite control gain as t approaches t_p. Additionally, there exist restricted regions in the system states for practical application. In the integrator backstepping technique, $z_{i+1}(t)$ is regarded as a control input for the i-th subsystem. If the desired virtual controllers exceed the constrained region, it is possible that $z_{i+1}(t)$ may face difficulties in tracking them [114].*

To address the previous two issues, we incorporate the following function to limit the control signals:

$$h_i(\sigma) = q_i^* \tanh\left(\frac{\sigma}{q_i^*}\right) = q_i^* \frac{e^{\sigma/q_i^*} - e^{-\sigma/q_i^*}}{e^{\sigma/q_i^*} + e^{-\sigma/q_i^*}} \tag{5.5}$$

where q_i^* is a positive constant. It is easy to show $h_i(\sigma)$ is a smooth bounded function that belongs to $(-q_i^*, q_i^*)$. Moreover, $h_i(\sigma)$ is differentiable at $\sigma = 0$ and can be transformed into the following equation by the mean-value theorem:

$$h_i(\sigma) = \frac{\partial h_i(\bar{\sigma})}{\partial \sigma}(\sigma - \sigma_0) + h_i(\sigma_0) \tag{5.6}$$

where $\bar{\sigma} \in (\sigma - \sigma_0)$, $\sigma_0 < \sigma$, and

$$\frac{\partial h_i(\bar{\sigma})}{\partial \sigma} = \frac{4}{(e^{\sigma/q_i^*} + e^{-\sigma/q_i^*})^2} \leq 1. \tag{5.7}$$

Furthermore, to simplify calculations, let us assume that $\sigma_0 = 0$. In this case, equation (5.6) can be represented as follows:

$$h_i(\sigma) = \frac{\partial h_i(\bar{\sigma})}{\partial \sigma}\sigma = h^*\sigma \tag{5.8}$$

where the positive constant h^* is chosen such that it satisfies the condition $0 < h_i^* \leq 1$.

5.2.1 Unmanned twin rotor helicopter model

The Quanser twin rotor helicopter model is being considered as depicted in Figure 5.1(a). The setup is mounted on a fixed base and comprises two propellers that are driven by DC motors. The front propellers are responsible for controlling the elevation of the twin rotor helicopter about the pitch axis, while the back propellers control the yaw angle. To control the pitch angle, a DC voltage (V_p) is applied to the DC motor associated with the front propellers. The design of V_p is carried out according to the desired pitch angle requirements. Similarly, the yaw angle of the

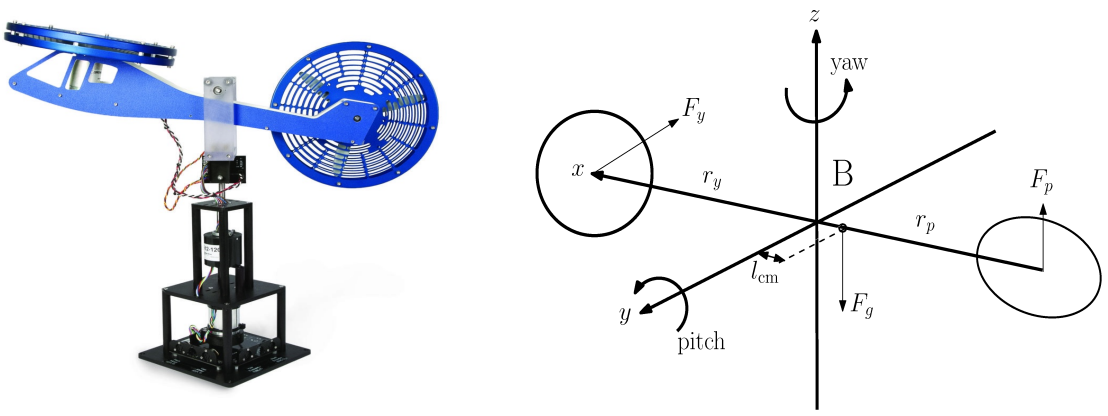

(a) (b)

Figure 5.1: Twin rotor helicopter: (a) Twin rotor helicopter platform structure. (b) Free-body diagram.

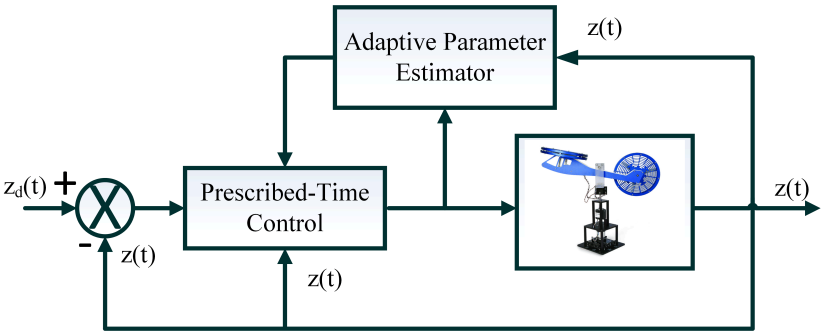

Figure 5.2: Illustration of the suggested control scheme.

twin rotor helicopter model is controlled by the back propellers, and the input V_y is designed to regulate the yaw angle. Pitch and yaw encoders are employed to measure the pitch and yaw angles of the twin rotor helicopter model. The pitch encoder and motor signals are transmitted via a slip ring, which eliminates the possibility of wires tangling on the yaw axis and allows for free rotation of the yaw angle within a range of 360 degrees. The yaw and pitch encoders are directly connected to a data-acquisition board, which provides the necessary position feedback for controlling the twin rotor helicopter. The data-acquisition board generates a control voltage that is amplified and used to drive the front and back motors. The front motor is driven by a Quanser Universal Power Module 2405 (UPM-2405), capable of supplying a maximum voltage of ±24V to the motors. On the other hand, the back motor is connected to a UPM-1503, which can deliver up to ±15V. Figure 5.1(b) illustrates the free-body diagram of the system, providing a visual representation of the forces and torques involved.

The equations of motion for the Quanser twin rotor helicopter, considered a rigid body, are

derived using the Euler-Lagrange equations, as presented in [44]. The resulting mathematical model is as follows:

The angular acceleration of the rotor in the θ direction, denoted by $\ddot{\theta}$, is given by the equation:

$$\begin{aligned}\ddot{\theta} = &- \frac{B_p\dot{\theta}}{J_p + m_h l^2} - \frac{m_h l^2 \dot{\psi}^2 \sin(\theta)\cos(\theta)}{J_p + m_h l^2} \\ &- \frac{m_h g l \cos(\theta)}{J_p + m_h l^2} + \frac{K_{pp}V_p}{J_p + m_h l^2} + \frac{K_{py}V_y}{J_p + m_h l^2}\end{aligned} \tag{5.9}$$

The angular acceleration of the rotor in the ψ direction, denoted by $\ddot{\psi}$, is given by the equation:

$$\begin{aligned}\ddot{\psi} = &\frac{2m_h l^2 \dot{\psi}\sin(\theta)\cos(\theta)\dot{\theta}}{J_y} - \frac{B_y\dot{\psi}}{J_y} \\ &+ \frac{K_{yp}V_p}{J_y} + \frac{K_{yy}V_y}{J_y}\end{aligned} \tag{5.10}$$

In the given context, the variables θ, $\dot{\theta}$, ψ, and $\dot{\psi}$ represent the pitch angle, pitch angular velocity, yaw angle, and yaw angular velocity, respectively. The input voltages applied to the pitch and yaw motors are denoted as V_p and V_y, respectively.

By rewriting the dynamic equations (5.9) and (7.5) in state space form, we can express them as follows:

$$\begin{cases} \dot{z}_1(t) = z_2(t) \\ \dot{z}_2(t) = \Theta_1^\top(z)\Phi_1 + b_p h_p(u_p) \\ \dot{z}_3(t) = z_4(t) \\ \dot{z}_4(t) = \Theta_2^\top(z)\Phi_2 + b_y h_y(u_y) \end{cases} \tag{5.11}$$

where, the state vector is $z(t)$ defined as:

$$\begin{bmatrix} z_1(t) \\ z_2(t) \\ z_3(t) \\ z_4(t) \end{bmatrix} = \begin{bmatrix} \theta \\ \dot{\theta} \\ \psi \\ \dot{\psi} \end{bmatrix} \tag{5.12}$$

and the control variables are defined as

$$\begin{bmatrix} u_1(t) \\ u_2(t) \end{bmatrix} = \begin{bmatrix} u_p(t) \\ u_y(t) \end{bmatrix} \tag{5.13}$$

where $u_p(t)$ and $u_y(t)$ represent the control inputs for the pitch and yaw motors, respectively, and are specified as:

$$u_p(t) = K_{pp}V_p + K_{py}V_y \tag{5.14}$$

$$u_y(t) = K_{yp}V_p + K_{yy}V_y \tag{5.15}$$

The functions Θ_1 and Θ_2 represent the matrices containing the known nonlinear terms in the dynamic equations, which can be specified as:

$$\Theta_1 = \begin{bmatrix} -z_2(t) \\ -\cos(z_1) \\ -z_4^2(t)\cos(z_1)\sin(z_1) \end{bmatrix},$$

$$\Theta_2 = \begin{bmatrix} -z_4(t) \\ z_2(t)z_4(t)\cos(z_1)\sin(z_1) \end{bmatrix}$$

Additionally, the vectors Φ_1 and Φ_2 are unknown constant vectors specified as

$$\Phi_1 = \begin{bmatrix} \frac{Bp}{J_p+m_h l^2} \\ \frac{m_h g l}{J_p+m_h l^2} \\ \frac{m_h l^2}{J_p+m_h l^2} \end{bmatrix},$$

$$\Phi_2 = \begin{bmatrix} \frac{B_y}{J_y} \\ \frac{2m_h l^2}{J_y} \end{bmatrix}$$

and the unknown input coefficients b_p and b_y are

$$b_p = \frac{1}{J_p + m_h l^2}, \quad b_y = \frac{1}{J_y}$$

Considering the objective of designing a control law for $u_1(t)$ and $u_2(t)$ in order to ensure that the state variables $z_1(t)$ and $z_3(t)$ track the reference trajectories $z_{d1}(t)$ and $z_{d3}(t)$ within a pre-specified time frame, the following assumptions are made:

Assumption 5 *For the twin rotor helicopter system model given by equation* (5.11)*, the unknown parameters* Φ_1*,* Φ_2*,* b_p*, and* b_y *are positive constants.*

Assumption 6 *For all* $t > 0$*, the desired reference tracking signals* $z_{d1}(t)$ *and* $z_{d2}(t)$ *are a smooth function of* t*, and their first and second-order derivative is known, piecewise continuous and bounded.*

Remark 5.5 *It is important to note that these assumptions are deemed reasonable and can be referenced in [44] for further details.*

5.3 Main results

The main results are organized into the following two parts: 5.3.1 introduces the design of a prescribed-time adaptive constraint feedback control for the unmanned twin rotor helicopter under consideration, and 5.3.2 presents the stability analysis associated with the control design.

5.3.1 Prescribed-time adaptive constraint feedback control design

For the unmanned twin rotor helicopter system under consideration, which involves uncertain parameters, we will employ an adaptive integrator backstepping methodology to design a prescribed-time constraint controller and adaptive laws. Figure 5.2 illustrates the block diagram of the proposed control methodology.

We begin by introducing the change of coordinates

$$x_1(t) = z_1(t) - z_{d1}(t) \tag{5.16}$$

$$x_2(t) = z_2(t) - h_1(\sigma_1) - \dot{z}_{d1}(t) \tag{5.17}$$

$$x_3(t) = z_3(t) - z_{d3}(t) \tag{5.18}$$

$$x_4(t) = z_4(t) - h_2(\sigma_2) - \dot{z}_{d3}(t) \tag{5.19}$$

where $\sigma_1(t)$ and $\sigma_2(t)$ are the virtual controllers, which are selected as:

$$\sigma_1(t) = -\gamma_1 \psi(t, t_p) x_1(t) \tag{5.20}$$

$$\sigma_2(t) = -\gamma_3 \psi(t, t_p) x_3(t) \tag{5.21}$$

where, γ_1 and γ_3 are positive design constants.

After the coordinate transformation, the dynamics of the system can be expressed as follows:

$$\begin{cases} \dot{x}_1(t) = x_2(t) + h_1(\sigma_1) \\ \dot{x}_2(t) = \Theta_1^\top(z)\Phi_1 + b_p h_p(u_p) - \dot{h}_1(\sigma_1) - \ddot{z}_{d1}(t) \\ \dot{x}_3(t) = x_4(t) + h_2(\sigma_2) \\ \dot{x}_4(t) = \Theta_2^\top(z)\Phi_2 + b_y h_y(u_y) - \dot{h}_2(\sigma_2) - \ddot{z}_{d3}(t) \end{cases} \tag{5.22}$$

Next, we put forward the following control law for achieving prescribed-time tracking of the system described by equation (5.22):

$$u_p(t) = \hat{\rho}_1 \bar{u}_p \tag{5.23}$$

$$u_y(t) = \hat{\rho}_2 \bar{u}_y \tag{5.24}$$

with

$$\begin{aligned} \bar{u}_p = &- a_1^* x_1(t) - a_1^* \Theta_1^\top(z)\hat{\Phi}_1 - \gamma_2 \psi(t, t_p) x_2(t) \\ &+ \dot{h}_1(\sigma_1) + \ddot{z}_{d1}(t) \\ \bar{u}_y = &- a_2^* x_3(t) - a_2^* \Theta_2^\top(z)\hat{\Phi}_2 - \gamma_4 \psi(t, t_p) x_4(t) \\ &+ \dot{h}_2(\sigma_2) + \ddot{z}_{d3}(t) \end{aligned}$$

Furthermore, the updating laws for the unknown parameters are chosen as follows:

$$\dot{\hat{\Phi}}_1 = \Xi_1 \Theta_1 x_2(t) \tag{5.25}$$

$$\dot{\hat{\Phi}}_2 = \Xi_2 \Theta_2 x_4(t) \tag{5.26}$$

$$\dot{\hat{\rho}}_1 = -\Upsilon_1 \bar{u}_p x_2(t) \tag{5.27}$$

$$\dot{\hat{\rho}}_1 = -\Upsilon_2 \bar{u}_y x_4(t) \tag{5.28}$$

where, a_1^* and a_2^* are positive constants chosen such that $a_1^* \geq \frac{1}{h_p^*}$ and $a_2^* \geq \frac{1}{h_y^*}$. The constants γ_2, γ_4, Υ_1, and Υ_2 are positive design constants. The matrices Ξ_1 and Ξ_2 are positive definite adaptive gain matrices. The variables $\hat{\Phi}_1$, $\hat{\Phi}_2$, $\hat{\rho}_1$, and $\hat{\rho}_2$ represent the estimates of Φ_1, Φ_2, $\rho_1 = \frac{1}{b_p}$, and $\rho_2 = \frac{1}{b_y}$, respectively.

Additionally, let $\tilde{\Phi}_1 = \Phi_1 - \hat{\Phi}_1$, $\tilde{\Phi}_2 = \Phi_2 - \hat{\Phi}_2$, $\tilde{\rho}_1 = \rho_1 - \hat{\rho}_1$, and $\tilde{\rho}_2 = \rho_2 - \hat{\rho}_2$ denote the parameter estimation errors.

5.3.2 Stability analysis

Theorem 5.6 *For the nonlinear system* (5.22) *with Assumption 5 and Assumption 6, under the proposed control law* (5.23) *and* (5.24) *along with the parameter updating law* (5.25), (5.26), (5.27), *and* (5.28), *the following conclusions can be made:*

- *All signals of the closed-loop system* (5.22) *remain bounded.*
- *The desired reference signals are accurately tracked within the prescribed time interval, i.e.*

$$\lim_{t \to T_p} \left[z_1(t) - z_{d1}(t) \right] = \lim_{t \to T_p} x_1(t) = 0$$

$$\lim_{t \to T_p} \left[z_3(t) - z_{d3}(t) \right] = \lim_{t \to T_p} x_3(t) = 0$$

Proof. Let us consider the candidate Lyapunov function as follows:

$$V(t) = V_1(t) + V_2(t) \tag{5.29}$$

where

$$\begin{aligned} V_1(t) =& \frac{1}{2} x_1^2(t) + \frac{1}{2} x_2^2(t) + \frac{1}{2} x_3^2(t) + \frac{1}{2} x_4^2(t) \\ V_2(t) =& \frac{1}{2} \tilde{\Phi}_1^\top \Xi_1^{-1} \tilde{\Phi}_1 + \frac{1}{2} \tilde{\Phi}_2^\top \Xi_2^{-1} \tilde{\Phi}_2 + \frac{b_p}{2\Upsilon_1} \tilde{\rho}_1^2 + \frac{b_y}{2\Upsilon_2} \tilde{\rho}_2^2 \end{aligned}$$

Now, let's take the time derivative of $V(t)$ along the solution to (5.22):

$$\begin{aligned} \dot{V}(t) =& x_1(t)\dot{x}_1(t) + x_2(t)\dot{x}_2(t) + x_3(t)\dot{x}_3(t) + x_4(t)\dot{x}_4(t) \\ & - \tilde{\Phi}_1^\top \Xi_1^{-1} \dot{\hat{\Phi}}_1 - \tilde{\Phi}_2^\top \Xi_2^{-1} \dot{\hat{\Phi}}_2 - \frac{b_p}{\Upsilon_1} \tilde{\rho}_1 \dot{\hat{\rho}}_1 - \frac{b_y}{\Upsilon_2} \tilde{\rho}_2 \dot{\hat{\rho}}_2 \end{aligned} \tag{5.30}$$

Table 5.1: Twin rotor helicopter parameters description.

Parameters	**Value**	**Unit**
Total moment of inertia about the pitch axis J_p	0.0384	$kg.m^2$
Total moment of inertia about the yaw axis J_y	0.0432	$kg.m^2$
Equivalent viscous damping coefficient about the pitch axis B_p	0.8	N/V
Equivalent viscous damping coefficient about the yaw axis B_y	0.318	N/V
The thrust force constant of yaw propeller K_{pp}	0.072	$N.m/V$
Thrust torque constant of yaw axis from yaw propeller K_{yy}	0.0068	$N.m/V$
Thrust torque constant acting on pitch axis from yaw propeller K_{py}	0.204	$N.m/V$
Thrust torque constant acting on yaw axis from pitch propeller K_{yp}	0.0219	$N.m/V$
Total moving mass of the helicopter (body, two propeller assemblies, etc.) m_h	1.3872	kg
Center of mass length along helicopter body from pitch axis l	0.1855	m
Acceleration due to gravity g	9.81	m/s^2
Maximum voltage applied to pitch motor V_{mp}	± 24	V
Maximum voltage applied to yaw motor V_{my}	± 15	V

Using (5.22), the time derivative $\dot{V}_1(t)$ can be expressed as:

$$\begin{aligned}\dot{V}(t) = {} & x_1(t)(x_2(t) + h_1(\sigma_1)) \\ & + x_2(t)\Big(\Theta_1^\top(z)\Phi_1 + b_p h_p(u_p) - \dot{h}_1(\sigma_1) - \ddot{z}_{d1}(t)\Big) \\ & + x_3(t)(x_4(t) + h_2(\sigma_2)) \\ & + x_4(t)\Big(\Theta_2^\top(z)\Phi_2 + b_y h_y(u_y) - \dot{h}_2(\sigma_2) - \ddot{z}_{d2}(t)\Big) \\ & - \tilde{\Phi}_1^\top \Xi_1^{-1}\dot{\hat{\Phi}}_1 - \tilde{\Phi}_2^\top \Xi_2^{-1}\dot{\hat{\Phi}}_2 - \frac{b_p}{\Upsilon_1}\tilde{\rho}_1\dot{\hat{\rho}}_1 - \frac{b_y}{\Upsilon_2}\tilde{\rho}_2\dot{\hat{\rho}}_2 \end{aligned} \tag{5.31}$$

Moreover, by using (5.8), we can rewrite the expression as:

$$x_1(t)h_1(\sigma_1) = x_1(t)\frac{\partial h_1(\bar{\sigma}_1)}{\partial \sigma_1}\sigma_1 \leq -h_1^*\gamma_1\psi(t,t_p)x_1^2(t) \tag{5.32}$$

$$x_2(t)b_p h_p(u_p) = x_2(t)\frac{\partial h_p(\bar{u}_p)}{\partial u_p}u_p \leq h_p^* b_p\hat{\rho}_1 x_2(t)\Bigg(- a_1^* x_1(t)$$

$$- a_1^*\Theta_1^\top(z)\hat{\Phi}_1 - \gamma_2\psi(t,t_p)x_2(t) + \dot{h}_1(\sigma_1) + \ddot{z}_{d1}(t)\Bigg) \tag{5.33}$$

$$x_3(t)h_2(\sigma_2) = x_3(t)\frac{\partial h_2(\bar{\sigma}_2)}{\partial \sigma_2}\sigma_2 \leq -h_2^*\gamma_3\psi(t,t_p)x_3^2(t) \tag{5.34}$$

$$x_4(t)b_y h_y(u_y) = x_4(t)\frac{\partial h_y(\bar{u}_y)}{\partial u_y}u_y \leq h_y^* b_y\hat{\rho}_2 x_4(t)\Bigg(- a_2^* x_3(t)$$

$$- a_2^*\Theta_2^\top(z)\hat{\Phi}_2 - \gamma_4\psi(t,t_p)x_4(t) + \dot{h}_2(\sigma_2) + \ddot{z}_{d3}(t)\Bigg) \tag{5.35}$$

Substituting (5.32)-(5.35) into (5.31), we obtain:

$$\begin{aligned}\dot{V}(t) \leq & - h_1^*\gamma_1\psi(t,t_p)x_1^2(t) - h_p^*\gamma_2\psi(t,t_p)x_2^2(t)\\ & - h_2^*\gamma_3\psi(t,t_p)x_3^2(t) - h_y^*\gamma_4\psi(t,t_p)x_4^2(t)\\ & + \Theta_1^\top\tilde{\Phi}_1 x_2(t) + \Theta_2^\top\tilde{\Phi}_2 x_4(t) - b_p\tilde{\rho}_1\bar{u}_p x_2(t)\\ & - b_y\tilde{\rho}_2\bar{u}_y x_4(t) - \tilde{\Phi}_1^\top\Xi_1^{-1}\dot{\hat{\Phi}}_1 - \tilde{\Phi}_2^\top\Xi_2^{-1}\dot{\hat{\Phi}}_2\\ & - \frac{b_p}{\Upsilon_1}\tilde{\rho}_1\dot{\hat{\rho}}_1 - \frac{b_y}{\Upsilon_2}\tilde{\rho}_2\dot{\hat{\rho}}_2\end{aligned} \tag{5.36}$$

By simplifying equation (5.36) even further, we can obtain:

$$\begin{aligned}\dot{V}(t) \leq & - h_1^*\gamma_1\psi(t,t_p)x_1^2(t) - h_p^*\gamma_2\psi(t,t_p)x_2^2(t)\\ & - h_2^*\gamma_3\psi(t,t_p)x_3^2(t) - h_y^*\gamma_4\psi(t,t_p)x_4^2(t)\\ & - \tilde{\Phi}_1^\top\Xi_1^{-1}\left(\dot{\hat{\Phi}}_1 - \Xi_1\Theta_1 x_2(t)\right)\\ & - \tilde{\Phi}_2^\top\Xi_2^{-1}\left(\dot{\hat{\Phi}}_2 - \Xi_2\Theta_2 x_4(t)\right)\\ & - \tilde{\rho}_1\frac{b_p}{\Upsilon_1}\left(\dot{\hat{\rho}}_1 + \Upsilon_1\bar{u}_p x_2(t)\right)\\ & - \tilde{\rho}_2\frac{b_y}{\Upsilon_2}\left(\dot{\hat{\rho}}_2 + \Upsilon_2\bar{u}_y x_4(t)\right)\end{aligned} \tag{5.37}$$

The parameters update laws (5.25), (5.26), (5.27), and (5.28) result in the cancellation of the last four terms in equation (5.37). Consequently, we are left with:

$$\begin{aligned}\dot{V}(t) \leq & - h_1^*\gamma_1\psi(t,t_p)x_1^2(t) - h_p^*\gamma_2\psi(t,t_p)x_2^2(t)\\ & - h_2^*\gamma_3\psi(t,t_p)x_3^2(t) - h_y^*\gamma_4\psi(t,t_p)x_4^2(t)\end{aligned} \tag{5.38}$$

Considering (5.29), (5.38) can be written as:

$$\dot{V}(t) \leq - \gamma\psi(t,t_p)V_1(t) \tag{5.39}$$

where $\gamma = \min\{2h_1^*\gamma_1, 2h_p^*\gamma_2, 2h_2^*\gamma_3, 2h_y^*\gamma_4\}$.

The prescribed-time stabilization of the unmanned twin rotor helicopter system, described by equations (5.9) and (5.10), can be directly inferred from Lemma 5.2 and equation (5.39). By applying the LaSalle-Yoshizawa theorem [105], it is guaranteed that $V(t)$ remains bounded. Consequently, this implies that $x_1(t)$, $x_2(t)$, $x_3(t)$, and $x_4(t)$ are also bounded and exhibit prescribed-time stability of the state. As t approaches t_p, $x_1(t)$, $x_2(t)$, $x_3(t)$, $x_4(t)$ converge to zero. Additionally, $\hat{\Phi}_1$ and $\hat{\Phi}_2$ are also bounded. Since $x_1(t) = z_1(t) - z_{d1}(t)$ and $x_3(t) = z_3(t) - z_{d3}(t)$, the tracking of the desired reference signal is attained within the prescribed time frame, t_p. Furthermore, $z_1(t)$ and $z_3(t)$ are bounded because $x_1(t)$ and $x_3(t)$ are bounded, and Assumption 6 guarantees that z_{d1} and $z_{d3}(t)$ are also bounded. By examining equations (5.20) and (5.21), it can be concluded that the virtual controls σ_1 and σ_2 are bounded. Additionally, from equations (5.23) and (5.24), it is evident that the control inputs can be ensured to remain bounded. This completes the proof. ■

5.4 Result discussion

In order to assess the efficacy of the adaptive prescribed-time constraint feedback control strategy developed in this study, we conducted a series of simulations and experiments. The primary objective was to validate the control strategy and analyze its performance under various conditions. Here, we present the results obtained from these simulations and experiments and provide a comprehensive discussion of the findings in this section.

5.4.1 Simulation results

We perform simulations to demonstrate and validate the effectiveness of the proposed adaptive prescribed-time constraint feedback control strategy and discuss the obtained results in this section. The parameters of the twin rotor helicopter system are given in Table 5.1. In this study, we set the initial conditions of the twin rotor helicopter as $z_1(0) = -20$ and $z_3(0) = 12$. The desired reference trajectory is taken as $z_{d1}(t) = 15\sin(2\pi 0.05t)$ and $z_{d3}(t) = 10\sin(2\pi 0.05t)$, which also fulfills Assumption 2. The design parameters are chosen as $\gamma_1 = 7$, $\gamma_2 = 10$, $\gamma_3 = 7$, $\gamma_4 = 10$, $\Xi_1 = \Xi_2 = 0.1$, $\Upsilon_1 = \Upsilon_2 = 0.02$. The constraint functions are chosen as $h_1(\sigma_1) = 10\tanh\left(\frac{\sigma_1}{10}\right)$, $h_p(u_p) = 24\tanh\left(\frac{u_p}{24}\right)$, $h_2(\sigma_2) = 8\tanh\left(\frac{\sigma_2}{8}\right)$, and $h_y(u_y) = 15\tanh\left(\frac{u_y}{15}\right)$. The simulations are performed considering the desired convergence time as $t_p = 10s$, i.e., the desired tracking should be achieved in $10s$.

The results from the simulation with the proposed prescribed-time adaptive constraint

feedback controller are shown in Figures 5.3-5.9. Figures 5.3 and 5.4 show that the desired pitch and yaw angle tracking is achieved in the prescribed-time $t_p = 10s$. The corresponding pitch angle and yaw angle tracking errors are shown in Figures 5.5 and 5.6, respectively. The estimate of parameters $\hat{\Phi}_1$ and $\hat{\Phi}_2$ are shown in Figure 5.7 and 5.8. Similarly, for prescribed-time $t_p = 10s$, the required input voltage plot is shown in Figure 5.9. From the obtained simulation results, one can conclude that the convergence is achieved within a priori chosen time. Moreover, all the closed-loop signals of the system are bounded.

5.4.2 Experimental results

We perform an experimental validation on Quanser's twin rotor helicopter platform based on the simulation results to verify the practical feasibility and effectiveness of the proposed adaptive prescribed-time-time constraint feedback control strategy. Figure 5.10 shows the experimental setup used for the experiments. Using the same reference signals and control parameter values as the simulation, we performed the experiments and the obtained experimental results are shown in Figures 5.11-5.15. Figures 5.11 and 5.12 show that the desired pitch and yaw angle tracking is achieved in the prescribed-time $t_p = 10s$. The corresponding pitch angle and yaw angle tracking errors are shown in Figures 5.13 and 5.14, respectively. Finally, for prescribed-time $t_p = 10s$, the required input voltage plot is shown in Figure 5.15. From the obtained experimental results, one can conclude that the convergence is achieved within a priori chosen time. Moreover, all the closed-loop signals of the system are bounded.

Remark 1 *As the obtained control law in this study is specifically designed for operation within the prescribed time t_p, ensuring continued tracking beyond t_p becomes crucial. To address this requirement and maintain control input throughout the system's operation, an alternative control law is applied for all $t > t_p$. In this case, we utilize the control law proposed in [112] to sustain effective control and tracking performance beyond the prescribed time. By incorporating this additional control law, we can extend the control capability and maintain desirable system behavior beyond the prescribed time horizon.*

5.5 Conclusion

In summary, we introduced a novel adaptive integrator backstepping controller with input constraints for an uncertain unmanned twin rotor helicopter. The controller is specifically designed to achieve reference trajectory tracking for the pitch and yaw angles within a predetermined

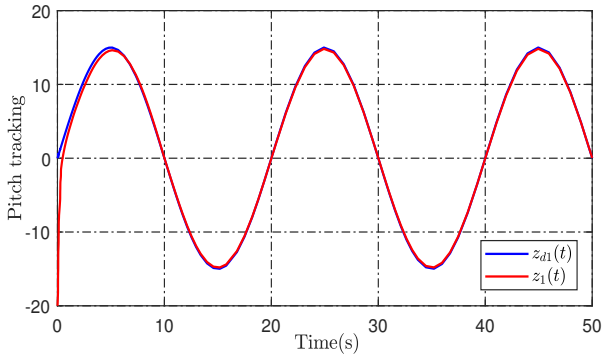

Figure 5.3: Desired pitch angle tracking with $t_p = 10s$.

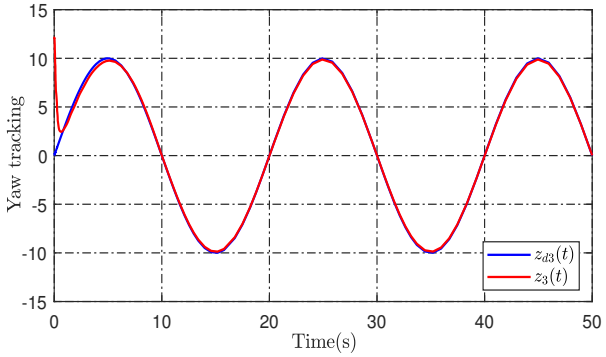

Figure 5.4: Desired yaw angle tracking with $t_p = 10s$.

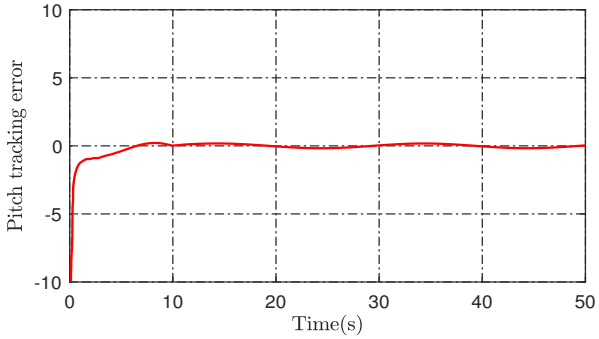

Figure 5.5: Pitch angle tracking error $x_1(t)$.

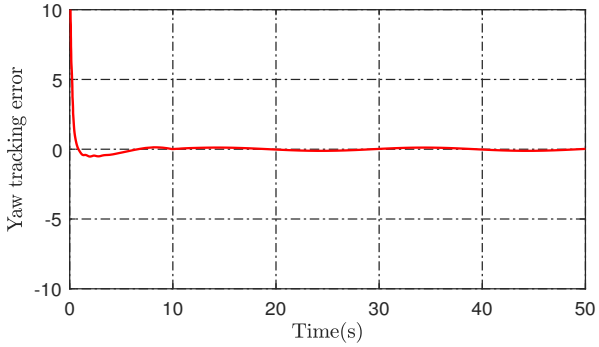

Figure 5.6: Yaw angle tracking error $x_3(t)$.

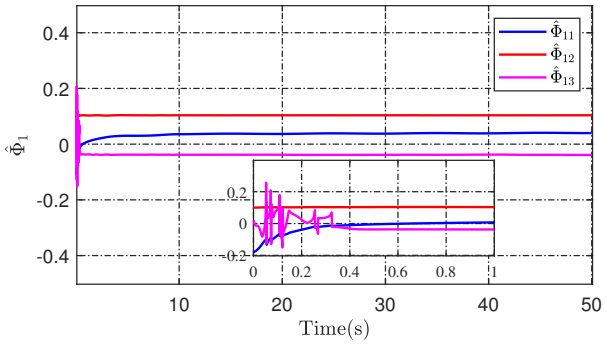

Figure 5.7: Estimate of $\hat{\Phi}_1$.

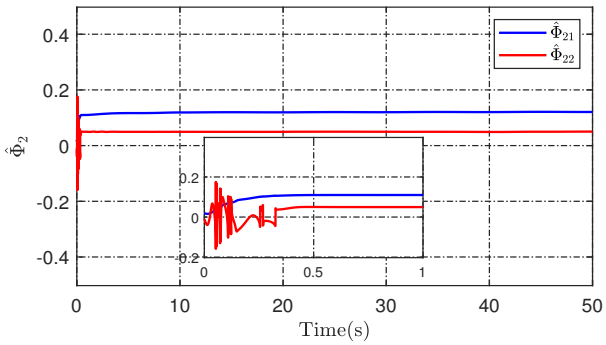

Figure 5.8: Estimate of $\hat{\Phi}_2$.

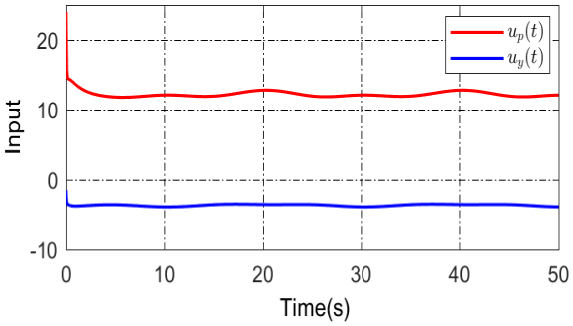

Figure 5.9: Required control inputs $u_p(t)$ and $u_y(t)$.

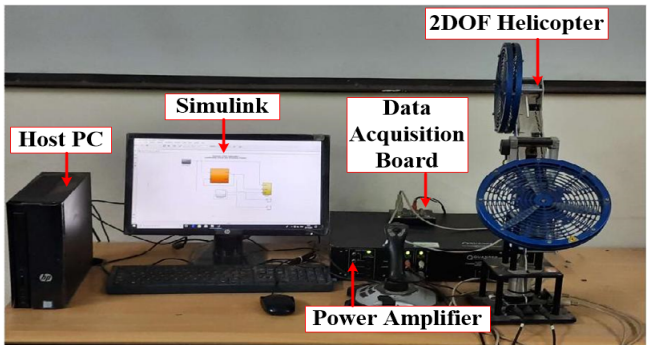

Figure 5.10: Twin rotor helicopter experimental setup.

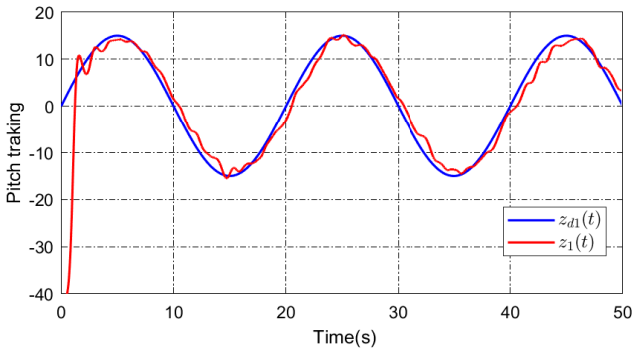

Figure 5.11: Desired pitch angle tracking with $t_p = 10s$.

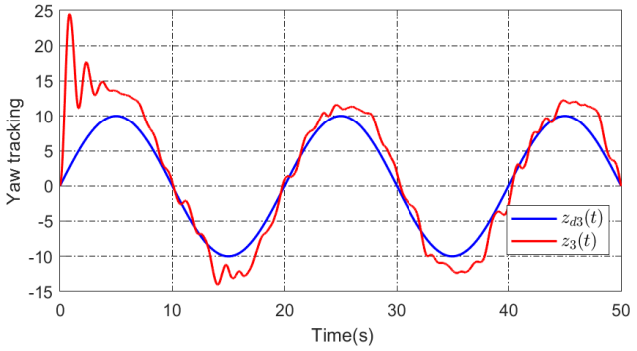

Figure 5.12: Desired yaw angle tracking with $t_p = 10s$.

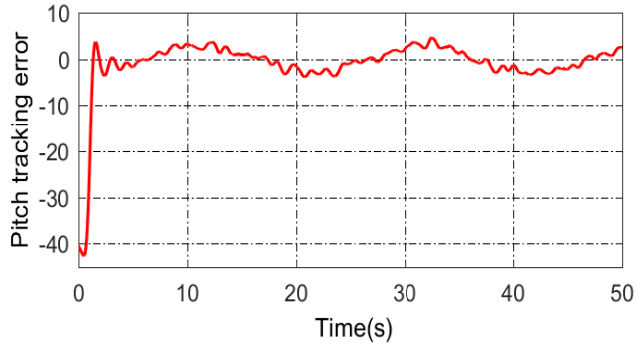

Figure 5.13: Pitch angle tracking error $x_1(t)$.

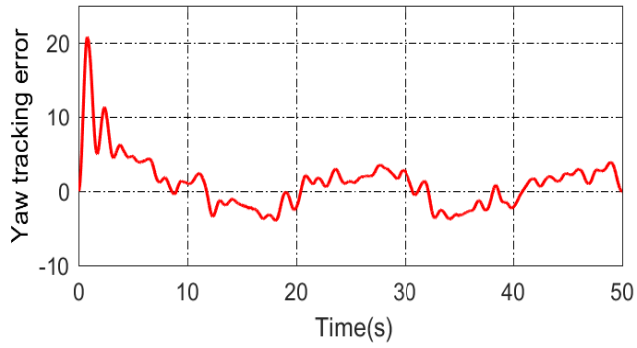

Figure 5.14: Yaw angle tracking error $x_3(t)$.

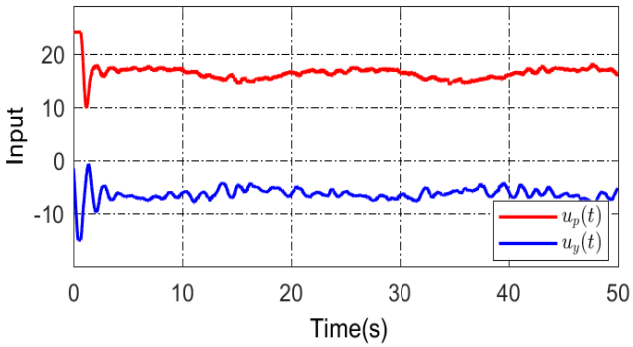

Figure 5.15: Required control inputs $u_p(t)$ and $u_y(t)$.

time frame. We derive the mathematical model of the twin rotor helicopter using the Euler-Lagrange equations and incorporate a constraint function to limit the virtual control signal as the terminal time approaches. Through the use of candidate Lyapunov functions and Lyapunov stability theory, we provide a theoretical proof of the proposed prescribed-time stabilization control achieved through adaptive integrator backstepping. Our analysis guarantees the boundedness of all signals within the closed-loop system and ensures the desired attitude tracking within the prescribed time frame. To validate the effectiveness and performance of our proposed control scheme, we conduct extensive simulations and experiments. The results obtained from these tests provide compelling evidence of the control potential and efficiency of our designed constraint-prescribed-time adaptive integrator backstepping controller.

In the next chapter, we extend adaptive prescribed-time control to regulate the output voltage of DC-DC boost converters within a predetermined time frame.